

## **Excitons and Davydov splitting in sexithiophene from first-principles many-body Green's function theory**

Xia Leng, Huabing Yin, Dongmei Liang, and Yuchen Ma

Citation: *The Journal of Chemical Physics* **143**, 114501 (2015); doi: 10.1063/1.4930975

View online: <http://dx.doi.org/10.1063/1.4930975>

View Table of Contents: <http://scitation.aip.org/content/aip/journal/jcp/143/11?ver=pdfcov>

Published by the AIP Publishing

---

### **Articles you may be interested in**

**Many-body effects and excitonic features in 2D biphenylene carbon**

*J. Chem. Phys.* **144**, 024702 (2016); 10.1063/1.4939273

**Quasiparticle electronic structure and optical absorption of diamond nanoparticles from ab initio many-body perturbation theory**

*J. Chem. Phys.* **140**, 214315 (2014); 10.1063/1.4880695

**Electronic excitations of bulk LiCl from many-body perturbation theory**

*J. Chem. Phys.* **139**, 214710 (2013); 10.1063/1.4835695

**Many-body Green's function GW and Bethe-Salpeter study of the optical excitations in a paradigmatic model dipeptide**

*J. Chem. Phys.* **139**, 194308 (2013); 10.1063/1.4830236

**Neutral and charged excitations in carbon fullerenes from first-principles many-body theories**

*J. Chem. Phys.* **129**, 084311 (2008); 10.1063/1.2973627

---



**NEW Special Topic Sections**

**NOW ONLINE**

Lithium Niobate Properties and Applications:  
Reviews of Emerging Trends

**AIP | Applied Physics  
Reviews**

# Excitons and Davydov splitting in sexithiophene from first-principles many-body Green's function theory

Xia Leng, Huabing Yin, Dongmei Liang, and Yuchen Ma<sup>a)</sup>

*School of Chemistry and Chemical Engineering, Shandong University,  
Jinan 250100, People's Republic of China*

(Received 28 May 2015; accepted 2 September 2015; published online 15 September 2015)

Organic semiconductors have promising and broad applications in optoelectronics. Understanding their electronic excited states is important to help us control their spectroscopic properties and performance of devices. There have been a large amount of experimental investigations on spectroscopies of organic semiconductors, but theoretical calculation from first principles on this respect is still limited. Here, we use density functional theory (DFT) and many-body Green's function theory, which includes the GW method and Bethe-Salpeter equation, to study the electronic excited-state properties and spectroscopies of one prototypical organic semiconductor, sexithiophene. The exciton energies of sexithiophene in both the gas and bulk crystalline phases are very sensitive to the exchange-correlation functionals used in DFT for ground-state structure relaxation. We investigated the influence of dynamical screening in the electron-hole interaction on exciton energies, which is found to be very pronounced for triplet excitons and has to be taken into account in first principles calculations. In the sexithiophene single crystal, the energy of the lowest triplet exciton is close to half the energy of the lowest singlet one. While lower-energy singlet and triplet excitons are intramolecular Frenkel excitons, higher-energy excitons are of intermolecular charge-transfer type. The calculated optical absorption spectra and Davydov splitting are in good agreement with experiments. © 2015 AIP Publishing LLC. [<http://dx.doi.org/10.1063/1.4930975>]

## I. INTRODUCTION

There are increasing attentions to linear  $\pi$ -conjugated organic semiconductors for their highly promising applications in electronics, photovoltaics, and spintronics.<sup>1–3</sup> Compared to their inorganic counterparts, organic semiconductors are more abundant, flexible, and lower-power consumption. Meanwhile, the electronic structures of organic semiconductors are more tunable.<sup>4</sup> Oligothiophene is one of the most important kinds of organic semiconductors and has been extensively studied for twofold reasons.<sup>5</sup> On the one hand, oligomers are more easily purified and their basic optoelectronic properties can be studied more precisely compared to polymers, which makes them better models than their parent polymers. On the other hand, on account of the restriction of high-level quantum chemistry methods to small systems, oligomers are an optimal choice to perform theoretical calculations from first principles than polymers.

A large effort has been devoted to characterize the optical and spectroscopic properties of oligothiophenes by experiments.<sup>6–9</sup> However, there remain many puzzling issues concerning, for example, the mechanism of Davydov splitting, charge transport, the lowest excited states, and size of excitons. Theoretical calculations from first principles may help us resolve these problems. But due to the huge size of the unit cell of oligothiophene single crystals, first principles calculations on their optical properties are still scarce. As a representative of the oligothiophene family, sexithiophene is a kind of active

material that have applications in light-emitting diodes and field-effect transistors.<sup>10,11</sup> The structure and optical spectra of sexithiophene single crystal have already been well defined by experiments.<sup>12–14</sup> Thus, sexithiophene presents itself as a good model for theoretical calculations and also offers an excellent testing ground for theoretical approaches.

In this work, we study the electronic excited states of sexithiophene molecule and crystal by a state-of-the-art *ab initio* method: many-body Green's function theory (MBGFT), including the GW method and Bethe-Salpeter equation (BSE).<sup>15–17</sup> Within MBGFT, electronic exchange and correlation effects are described by the electron self-energy operator within Hedin's GW approximation, accompanied by solving the BSE of correlated electron-hole ( $e-h$ ) excitations. The GW+BSE approach has become a standard procedure for optical excitation calculations in many systems including clusters, molecules, and crystals.<sup>18–20</sup> It has also been used to study the excitons in organic semiconductors, such as pentacene, picene, polythiophene, and PTCDA.<sup>4,21,22</sup>

Tamm-Danoff approximation (TDA) and static screening limit in the  $e-h$  interaction are usually applied in routine BSE calculations. In this work, we tested their validity in sexithiophene. Especially, we will show that static screening approximation may lead to large errors in the energies of triplet excitons. In this case, dynamical screening effects must be taken into account. Singlet exciton fission, in which a singlet exciton splits into two triplet ones, attracts great attention recently since it is expected to be a promising way to increase the efficiency of photovoltaic devices.<sup>23,24</sup> Many theoretical works have been done to compare the energy levels

<sup>a)</sup>Electronic mail: myc@sdu.edu.cn

of singlet and triplet excited states for organic semiconductors, especially pentacene.<sup>25–29</sup> We found that in sexithiophene crystal the energy of the lowest triplet excited state becomes close to half the energy of the lowest singlet one if dynamical screening effects in the *e-h* interaction are considered. By comparing the *b*-polarized and *c*-polarized optical absorption spectra of sexithiophene crystal, we identify the Davydov splitting to be 0.36 eV, which is in excellent agreement with experiments.<sup>13,30</sup> Here, we will also discuss the size of singlet and triplet excitons, which is important for charge transport and energy transfer.

The paper is organized as follows. Section II contains the basic ingredients of the many-body Green's function theory and the technical details in our calculations. In Sec. III, we discuss the singlet and triplet excited states of the gas-phase sexithiophene molecule. The results and discussions on the sexithiophene single crystal are given in Sec. IV.

## II. THEORY AND METHOD

### A. Ground state

Ground-state geometries of sexithiophene molecule and crystal are relaxed by density-functional theory (DFT). We employed three types of exchange-correlation (XC) functionals, including the standard generalized gradient approximation of Perdew-Burke-Ernzerhof (PBE),<sup>31</sup> the hybrid functional of Becke-3-Lee-Yang-Parr (B3LYP),<sup>32,33</sup> and the Coulomb-attenuating method applied to B3LYP (CAM-B3LYP),<sup>34</sup> for the molecule by the GAUSSIAN09 code.<sup>35</sup> The molecule geometry depends strongly on the XC type. By PBE and B3LYP, the molecule is planar. By CAM-B3LYP, the dihedral angles between adjacent thiophene rings are around 30°, leading to a nonplanar structure as shown in Fig. 1(a).

The crystal structure of sexithiophene is monoclinic (symmetry  $P2_1/n$ ) with four molecules in the unit cell (see

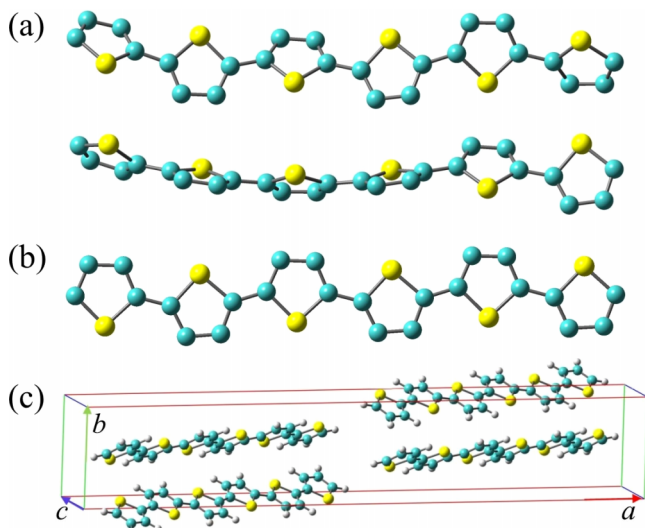


FIG. 1. Structures of the sexithiophene molecule and crystal: (a) the nonplanar structure of the molecule optimized by DFT-CAM-B3LYP from top and side views. (b) The planar structure of the molecule optimized by DFT-PBE. (c) The structure of the crystal with four molecules in the unit cell. *a*, *b*, and *c* denote crystal axes.

Fig. 1(c)).<sup>12</sup> Sexithiophene molecule is planar in the bulk crystal. In our calculations, the lattice parameters are set to those measured in experiment, i.e.,  $a = 44.708 \text{ \AA}$ ,  $b = 7.851 \text{ \AA}$ ,  $c = 6.029 \text{ \AA}$ ,  $\alpha = 90.0^\circ$ ,  $\beta = 90.76^\circ$ , and  $\gamma = 90.0^\circ$ .<sup>12</sup> Initial coordinates of atoms in the unit cell are set to the experimental values in Ref. 12, which are then optimized within DFT by the SIESTA code<sup>36</sup> using the PBE exchange-correlation functional with double  $\zeta$  plus a single shell of polarization function as basis set. We use a *k*-point mesh of  $1 \times 3 \times 3$ . The C–C and C–S bond lengths after optimization are 0.02–0.04 Å longer than those measured by experiment.

### B. GW method

It is well-known that DFT usually fails to correctly predict the band structures of solids and electronic levels of molecules, especially when using standard local and semilocal approximations to the XC potential. MBGFT, typically based on DFT calculations as a starting point, has become a standard approach to compute electronic structures that are in excellent agreement with experiment. Within MBGFT, electronic structures are calculated through the quasiparticle (QP) equation,<sup>37,38</sup>

$$\left\{ -\frac{\hbar^2}{2m} \nabla^2 + V_{ps}(\mathbf{r}) + V_H(\mathbf{r}) \right\} \psi_{n\mathbf{k}}^{QP}(\mathbf{r}) + \int \Sigma(\mathbf{r}, \mathbf{r}', E_{n\mathbf{k}}^{QP}) \psi_{n\mathbf{k}}^{QP}(\mathbf{r}') d\mathbf{r}' = E_{n\mathbf{k}}^{QP} \psi_{n\mathbf{k}}^{QP}(\mathbf{r}). \quad (1)$$

$\Sigma(\mathbf{r}, \mathbf{r}', E)$  is the nonlocal, energy-dependent self-energy operator, which describes the exchange-correlation interactions among electrons. In the GW method proposed by Hedin and Lundqvist,<sup>37,38</sup>  $\Sigma(\mathbf{r}, \mathbf{r}', E)$  can be evaluated by

$$\Sigma(\mathbf{r}, \mathbf{r}', E) = \frac{i}{2\pi} \int e^{-i\omega 0^+} G(\mathbf{r}, \mathbf{r}', E - \omega) W(\mathbf{r}, \mathbf{r}', \omega) d\omega, \quad (2)$$

where  $G$  and  $W$  are the one-body Green function and the screened Coulomb interaction, respectively. The static part  $W(\omega = 0)$  is calculated using the random-phase approximation, while the dynamic part  $W(\omega \neq 0)$  is calculated using the plasmon-pole model (PPM).<sup>39</sup> In this work, GW calculations are performed by the one-shot  $G_0W_0$  method. However, in the calculations of dielectric function and Green's function, a scissor shift is applied to the DFT energies of unoccupied orbitals. The scissor shift is adjusted until it equals the difference between the quasiparticle band gap and the DFT one.

### C. Bethe-Salpeter equation

For singlet-to-singlet excitations, the generalized BSE takes the form<sup>15</sup>

$$\begin{pmatrix} R & C \\ -C^* & -R^* \end{pmatrix} \begin{pmatrix} A \\ B \end{pmatrix} = \Omega \begin{pmatrix} A \\ B \end{pmatrix}, \quad (3)$$

with  $R = D + 2K^{R,x} + K^{R,d}$ ,  $C = 2K^{C,x} + K^{C,d}$ , and  $D \equiv (E_c^{QP} - E_v^{QP})$ .<sup>16</sup>  $R$  and  $-R^*$  are the Hamiltonians corresponding to the resonant ( $v \rightarrow c$ ) and the antiresonant ( $c \rightarrow v$ ) parts of the transitions, respectively, while  $C$  and  $-C^*$  are the coupling terms between the resonant and antiresonant transitions.  $K^{R,x}$  ( $K^{R,d}$ ) and  $K^{C,x}$  ( $K^{C,d}$ ) are the bare exchange term (screened direct term) of the *e-h* interaction kernel for

the resonant transition and the corresponding coupling terms, respectively.  $E_c^{QP}$  and  $E_v^{QP}$  are the quasiparticle energies for the unoccupied (conduction) and occupied (valence) orbitals, respectively.  $\Omega$  is the excitation energy. Within the Tamm-Danoff approximation,  $C$  is assumed to be zero; this is a good approximation for cases where the coupling terms

are much smaller than the resonant and antiresonant terms. For singlet-to-triplet excitations, terms  $R$  and  $C$  in Eq. (3) become  $R = D + K^{R,d}$  and  $C = K^{C,d}$ , respectively, with the bare exchange contributions removed.

Within PPM, the direct interaction of the resonant transition  $K^{R,d}$  is calculated by<sup>16</sup>

$$K_{vc,v'c'}^{R,d}(\Omega) = - \sum_l \int d\mathbf{r} d\mathbf{r}' \psi_c^*(\mathbf{r}) \psi_{c'}(\mathbf{r}) \psi_v(\mathbf{r}') \psi_{v'}^*(\mathbf{r}') W_l(\mathbf{r}, \mathbf{r}') \\ \times \frac{z_l \omega_l}{2} \left[ \frac{1}{\omega_l - (\Omega - (E_{c'}^{QP} - E_{v'}^{QP}))} + \frac{1}{\omega_l - (\Omega - (E_c^{QP} - E_v^{QP}))} \right], \quad (4)$$

where  $\omega_l$  is the plasmon frequency and  $W_l(\mathbf{r}, \mathbf{r}')$  is the spatial behavior of the screened interaction at the plasmon mode  $l$ . The matrix elements of  $K^{C,d}$  have a similar form. The direct interaction is responsible for the binding between electron and hole in the exciton. The static screening (i.e., approximating both energy denominators in Eq. (4) to  $\omega_l$ ) constitutes the main part of the  $e-h$  attraction, while the dynamical effects are usually much smaller and can thus be considered as a perturbation to the results from static screening. The dynamical effects can be neglected when the excitonic binding energies, i.e., the absolute values of terms  $\Omega - (E_c^{QP} - E_v^{QP})$  in Eq. (4), are much smaller than the characteristic plasma frequencies  $\omega_l$ . The BSE including dynamical effects can be solved approximately through first order perturbation theory,<sup>40</sup> i.e., by

$$\delta\Omega = \sum_{vcv'c'} A_{vc}^* [K_{vc,v'c'}^{R,d}(\Omega) - K_{vc,v'c'}^{R,d}(\text{static})] A_{v'c'}. \quad (5)$$

Note that the underlying GW single-particle levels are calculated from dynamical screening in all cases.

Kohn-Sham eigenvalues and eigenwave functions are needed to construct the operators in GW and BSE. In this work, for all the geometries, we only use DFT with the PBE functional to get these quantities. We have tested that changing PBE to other type of functionals, such as Ceperley-Alder of local density approximation and BLYP, has little effect on excitation energies. The basis sets for GW, BSE, and the underlying DFT calculations are expressed in terms of atom-centered Gaussian orbitals of the form<sup>17</sup>

$$\phi_{ijk}(\mathbf{r}) = A_{ijk} x^i y^j z^k e^{-\alpha r^2}. \quad (6)$$

For each procedure, four decay constants ( $\alpha$ ) are used for C and S atoms (0.2, 0.5, 1.25, and 3.2 in a.u.), and three decay constants are used for H atoms (0.1, 0.4, and 1.5 in a.u.). For DFT, the basis set includes  $s$ ,  $p$ , and  $d$  orbitals, while for GW and BSE, orbitals of  $f$  symmetry are also included as explained in Ref. 17. The decay constants were optimized with the density fitting approach. They have been well tested to yield converged orbital energies and excitation energies. These sets of decay constants have also been applied in the previous GW+BSE calculations on organic systems, e.g., DNA, RNA, and biological chromophores.<sup>40-43</sup>

### III. SEXITHIOPHENE MOLECULE

We first studied the gas-phase sexithiophene molecule. Table I lists the energies of the lowest singlet and triplet excitons of sexithiophene molecule based on the geometries relaxed by three different XC potentials. The lowest absorption peak of sexithiophene molecule is composed by the lowest singlet exciton. The geometries from B3LYP and PBE are both planar, with difference in the C–C and C–S bond length in the range of 0.01–0.02 Å. This makes the excitation energies from B3LYP and PBE geometries differ by about 0.15 eV. By CAM-B3LYP, the geometry of the molecule is highly twisted, and the excitation energies are significantly higher than those from PBE and B3LYP.

Within TDA and static screening limit of the  $e-h$  interaction, the absorption peaks calculated from the three geometries deviate from the experimental value by 0.28 eV

TABLE I. The lowest singlet and triplet excitation energies (in eV) of sexithiophene molecule in the gas phase calculated by the GW+BSE approach under different approximations at the geometries optimized by DFT employing exchange-correlation functionals of CAM-B3LYP, B3LYP, and PBE. The second, third, and fourth columns refer to calculations within the Tamm-Danoff approximation (“TDA”), while the fifth and sixth columns are from full BSE calculations which take into account the resonant-antiresonant coupling (cf. Eq. (3)). “sta.” and “dyn.” denote BSE calculations within the static screening limit and with dynamical screening effects considered in the electron-hole interaction, respectively. “1st” and “diag.” represent that the dynamical screening effects are calculated by first-order perturbation theory and by diagonalizing the updated BSE Hamiltonian, respectively. (The lowest singlet excitation energy is at 2.85 eV by experiment.<sup>9</sup>)

Geometry	TDA			Full BSE	
	sta.	dyn.(1st)	dyn.(diag.)	sta.	dyn.(1st)
Singlet					
CAM-B3LYP	3.13	3.01	2.99	3.03	2.91
B3LYP	2.50	2.40	2.38	2.39	2.30
PBE	2.36	2.27	2.26	2.20	2.11
Triplet					
CAM-B3LYP	2.05	1.72	1.67	1.94	1.60
B3LYP	1.38	1.11	1.05	1.26	0.97
PBE	1.20	0.95	0.89	1.00	0.71

at least. When we went beyond TDA, i.e., solving the full BSE by taking into account the coupling terms in Eq. (3), the excitation energies redshift by about 0.1 eV. Considering further dynamical screening effects in the  $e-h$  interaction into full BSE through the procedure mentioned in Section II, the excitation energies redshift by another 0.1 eV. Now the energy of the lowest absorption peak is at 2.91 eV at the CAM-B3LYP geometry, which is very close to the experimental value of 2.85 eV.<sup>9</sup> Considering the success of GW+BSE method in other organic molecules,<sup>19,40,42,43</sup> we can come to the conclusion that sexithiophene molecule takes the nonplanar CAM-B3LYP geometry in the gas phase. Quantum chemistry calculations have also proved that DFT relaxation at the CAM-B3LYP level usually gives better ground-state structures than PBE and B3LYP.<sup>44,45</sup> The second lowest excited state of the sexithiophene molecule is dipole-forbidden and is 0.7 eV higher in energy than the lowest one. It has no contribution to the absorption peak.

For triplet excitons, TDA also overestimates the energies by about 0.1 eV (see Table I), the same as the singlets. The magnitude of dynamical screening correction to the energy for triplet excitons is nearly three times larger than that for singlet ones. Nearly, all the dynamical screening correction comes from  $K^{R,d}$  in the diagonal terms of Eq. (3), while contribution from  $K^{C,d}$  in the off-diagonal terms is negligible. From Eq. (4), the magnitude of dynamical screening effects depends on the exciton binding energies ( $E_c^{QP} - E_v^{QP}$ ) -  $\Omega$ . The larger the exciton binding energies are, the stronger the dynamical screening effects are. Exciton binding energies of triplet excitons are larger than those of singlet ones by 1 eV. This makes the dynamical screening correction to the triplet excitons larger than that to the singlet ones. The lowest singlet and triplet excitons of the sexithiophene molecule are both mainly composed by the transition from the highest molecular orbital (HOMO/H) to the lowest unoccupied molecular orbital (LUMO/L). At the CAM-B3LYP geometry, the matrix element of  $K_{H,L;H,L}^{R,d} = -3.0$  eV,  $K_{H,L;H,L}^{R,x} = 0.4$  eV. The magnitude of  $K^{R,d}$  is so large that several percent improvement on it can induce several tenths of eV in the excitation energy.

The dynamical screening corrections presented above are calculated through first-order perturbation theory as discussed in Section II. This may be accurate enough for singlet excitons where the corrections are small (~0.1 eV). For triplet excitons, we need to check its validity due to the large dynamical screening corrections (~0.3 eV) compared to the exciton energies (e.g., ~2.0 eV at the CAM-B3LYP geometry, ~1.0 eV at the PBE geometry). We did this as follows. After obtaining the exciton energies at the static screening limit of the  $e-h$  interaction, matrix elements of the direct interaction  $K^d$  were recalculated by inserting exciton energies into Eq. (4). Eigenvalues of the updated BSE Hamiltonian with dynamical screening effects taken into account were then evaluated through direct diagonalization. We found that energies of the triplet excitons are further redshifted by about 0.06 eV compared to those calculated by first-order perturbation theory (see Table I).

The singlet-triplet splittings from TDA to full BSE change little as can be seen from Table I. Recent theoretical calculations show that serious triplet instability problem may occur when applying time-dependent density functional theory

(TDDFT) on organic molecules like butadiene, naphthalene, anthracene, dimethylaminobenzonitrile, and polyacetylene oligomers, while TDA can alleviate this problem.<sup>46,47</sup> This difference between MBGFT and TDDFT needs to be studied in the future.

#### IV. SEXITHIOPHENE CRYSTAL

In the GW+BSE calculations for sexithiophene crystal the unit cell of which contains 176 atoms, we use  $k$ -point meshes of  $1 \times 2 \times 2$  to set up the matrix elements of dielectric function and self-energy operator, and  $1 \times 7 \times 7$  to describe the excited state. These  $k$ -point samplings can give converged results for both quasiparticle energies and optical spectrum. Occupied (unoccupied) states that are within 2.5 eV to the valence band maximum (conduction band minimum) are included in the BSE calculation, which is enough to model the low-energy excited states we are interested in with high accuracy.

The dielectric constant of sexithiophene crystal is calculated to be 4.3, which is in agreement with experiments.<sup>48–50</sup> Fig. 2 gives the band structures of sexithiophene crystal calculated by DFT and GW approaches. From DFT to GW, dispersion of the bands changes little. The band gap is enlarged by 1.3 eV. The spacing between valence bands and that between conduction bands is also enlarged in GW calculations. For example, the spacing between bands  $a$  and  $b$  and that between bands  $c$  and  $d$  in GW increases by ~30% compared to the counterparts in DFT.

The optical absorption spectra calculated by GW+BSE and the corresponding experimental spectra are summarized in Fig. 3 for polarization along the  $b$  and  $c$  crystal axes with light propagating along the  $a$  crystal axis. These two polarization directions have been heavily investigated by experiments. For comparison, the spectrum for polarization along the  $a$  axis with light propagating along the  $b$  axis is also shown in Fig. 3. Note that, to make a better guideline for comparison between calculated and experimental spectra, the energy axis of the experimental spectra in Fig. 3(c) is shifted by 0.3 eV relative

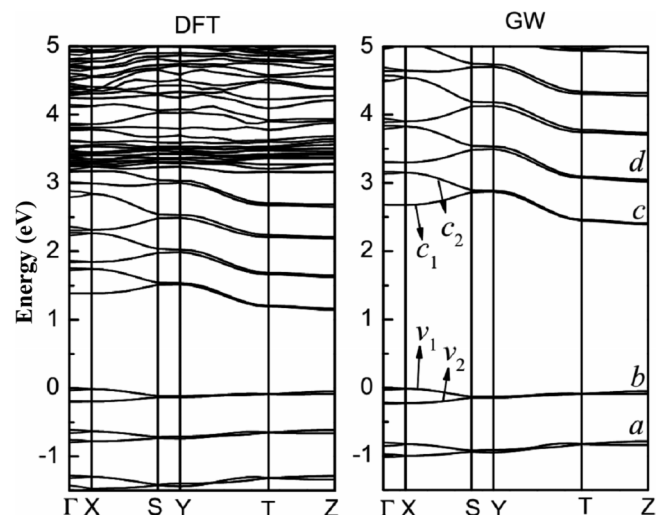


FIG. 2. Band structures of sexithiophene crystal calculated by DFT and GW method.  $v_1$ ,  $v_2$ ,  $c_1$ , and  $c_2$  denote the highest two valence bands and the lowest two conduction bands.

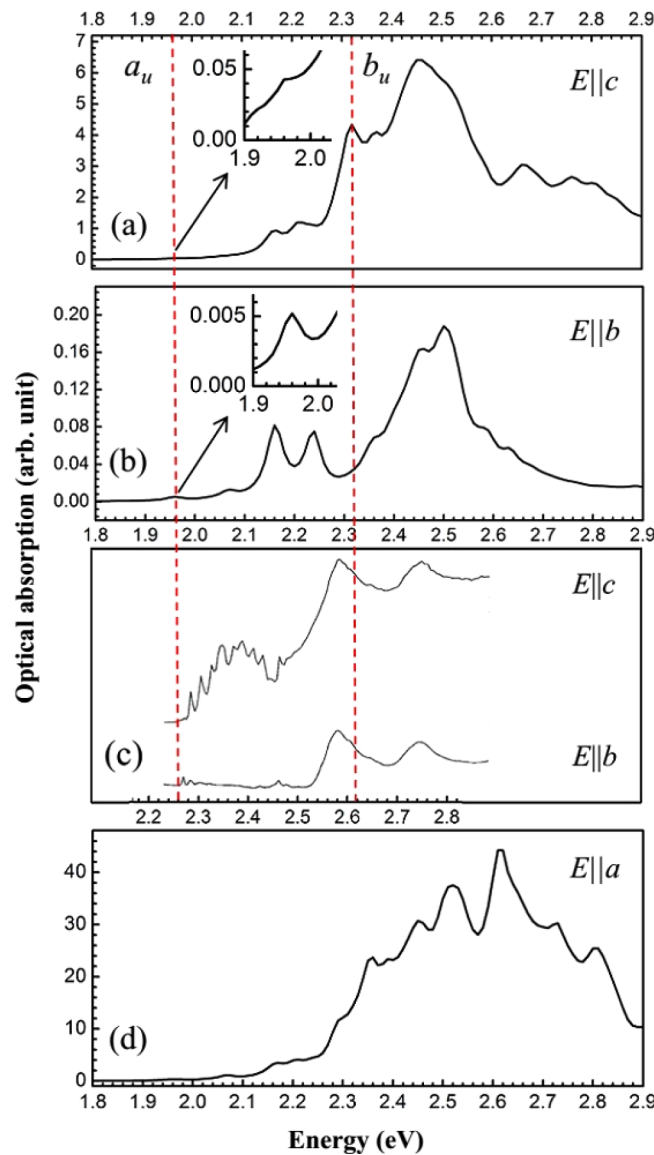


FIG. 3. Optical absorption spectra of sexithiophene crystal with light polarized along the  $b$  ( $E \parallel b$ ),  $c$  ( $E \parallel c$ ), and  $a$  ( $E \parallel a$ ) axes. (a), (b), and (d) are the calculated spectra by GW+BSE with an artificial Gaussian broadening of 0.02 eV. Experimental spectra from Ref. 13 are given in (c) for a comparison. Red dashed lines indicate the position of the  $a_u$  and  $b_u$  Davydov components from our calculations. The insets of (a) and (b) show the enlarged views of the regions indicated by arrows.

to those in Figs. 3(a) and 3(b). Some factors can influence the precision of the calculated spectra when compared to the experiment.

First, the geometry of sexithiophene molecule in the theoretical crystal model calculated by DFT-PBE is a little different from that measured by experiment. The C-C and C-S bonds in the former are 0.02–0.04 Å longer than those in the latter as have been discussed in Section II A. We compared the excited states of isolated sexithiophene molecules at the geometries extracted from the theoretical crystal model and from the experiment. Excitation energies in the former are 0.4 eV lower than those in the latter.

Second, the spectra in Figs. 3(a) and 3(b) are calculated within the Tamm-Dancoff approximation and static screening

limit in the  $e-h$  interaction. As discussed in Section II, these two approximations can cause 0.2 eV redshift of the energies of lower singlet excited states. As will be discussed in detail later in this section, we estimate that these two approximations can also lead to 0.2 eV redshift of the absorption spectra of the sexithiophene crystal.

Taking the above two factors into account, the calculated spectra shown in Figs. 3(a) and 3(b) should be blueshifted by about 0.2 eV, which are then in more agreement with the experimental spectra in Fig. 3(c). Recent theoretical work demonstrates that electron-phonon coupling can affect strongly the optical and electronic properties of carbon-based materials such as trans-polyacetylene, bulk diamond, and diamond nanoparticles in the respects of both optical absorption energies and lineshapes.<sup>51–53</sup> The experimental spectra in Fig. 3(c) also involve vibronic bands, such as the narrow peaks between 2.3 eV and 2.5 eV for the  $c$ -polarized spectrum. These lattice vibration effects influence the strength of the optical absorption, which is beyond the scope of our present work and the capability of MBGFT without electron-phonon interaction taking into account. Furthermore, defects, impurities, and disorder in the crystal may create additional absorption lines in the energy region we are interested in Refs. 30 and 54–57.

The sexithiophene crystal consists of two sublattices that are not connected by a simple translation, which causes the Davydov splitting. The lowest singlet excited state of the isolated sexithiophene molecule is  $1^1B_u$ . In the crystal, it splits into four levels,  $a_u$ ,  $a_g$ ,  $b_u$ , and  $b_g$ , of which  $a_u$  and  $b_u$  are dipole allowed while the others dipole forbidden. Previous theoretical calculations based on the Ewald dipole sums predict that  $a_u$  is weakly allowed and completely  $b$ -polarized, while  $b_u$  is strongly allowed and polarized in the  $ac$  crystal plane and should not be observed under  $b$ -polarized light irradiation.<sup>30,54,58</sup> According to this and experimental spectra, energies of the  $a_u$  and  $b_u$  Davydov components have been determined to be 2.28 and 2.60 eV, respectively, with a Davydov splitting of 0.32 eV.<sup>13,30</sup>

According to our GW+BSE calculations, the lowest two singlet excitons of sexithiophene crystal are degenerate at the energy of 1.96 eV, which can be assigned to the levels  $a_u$  and  $a_g$ . These two excitons are totally Frenkel states with the excitons localized in a single molecule as shown in Fig. 4(a) for the spatial distribution of the exciton. The exciton binding energy of them is 0.7 eV. In the gas-phase sexithiophene molecule, the typical exciton binding energy is 3 eV. The ratio of the Frenkel exciton binding energies in the gas and bulk crystal phases equals approximately the dielectric constant which is calculated to be 4.3. This drastic reduction of exciton binding energy from isolated organic molecule to the corresponding bulk phase induced by the intermolecular screening has also been found in the previous GW+BSE calculations on polymers by van der Horst *et al.*<sup>59,60</sup> The level  $a_u$  creates a weakly absorption peak which can be discerned in the  $b$ -polarized spectrum (Fig. 3(b)) but is undetectable in the  $c$ -polarized spectrum (Fig. 3(a)). This is in agreement with experiment. A sharp difference between the  $c$ - and  $b$ -polarized spectra emerges at 2.32 eV, where there is a strong peak in the former but not in the latter. The excitation at 2.32 eV can be assigned

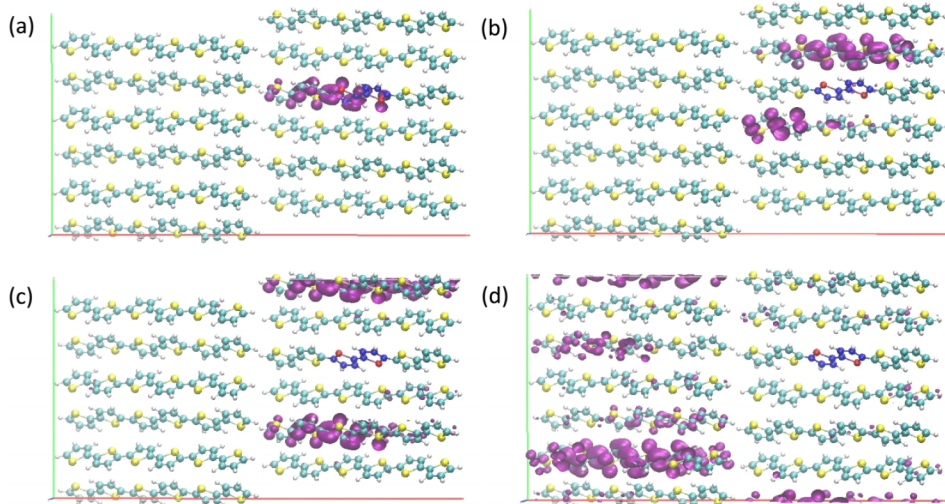


FIG. 4. Electronic charge distribution (purple solid surface) for singlet excitons at the energies of 1.96 (a), 2.16 (b), 2.32 (c), and 2.45 eV (d) in a sexithiophene crystal  $1 \times 3 \times 1$  supercell. The hole is fixed near the atoms represented by blue and red balls which are carbon and sulfur atoms, respectively. While it is a Frenkel exciton at 1.96 eV, it is a charge-transfer exciton at the other cases.

to the  $b_u$  Davydov component according to the discussion in the last paragraph. The Davydov splitting is thus 0.36 eV from our calculations, which agrees with experiment. The exciton of the  $b_u$  level is of charge-transfer type (see Fig. 4(c)), where the excited electron jumps in the direction along the  $bc$  plane to adjacent sexithiophene molecules of the same sublattice. The exciton binding energy of  $b_u$  is 0.3 eV, half that of  $a_u$ .

The prominent peaks at 2.45 eV in both  $c$ - and  $b$ -polarized spectra (Figs. 3(a) and 3(b)) should correspond to the peaks at 2.76 eV in the experimental spectra (Fig. 3(c)). They also originate from charge-transfer transitions, as shown in Fig. 4(d) for one charge-transfer pathway that contributes to these peaks. There are also two obvious peaks at 2.16 and 2.21 eV in both Figs. 3(a) and 3(b), which may be related to the peaks at around 2.48 eV observed in experiment (Fig. 3(c)). These two peaks also originate from charge-transfer transitions, where the excited electron jumps in the direction along the  $bc$  plane to the nearest-neighbor molecules of different sublattices as shown in Fig. 4(b) for the exciton at 2.16 eV. The exciton binding energies for these two peaks are 0.5 eV, relatively larger than that for  $b_u$ . All the excited states between  $a_u$  and 2.45 eV discussed above are composed of transitions between the highest two valence bands and the lowest two conduction bands ( $v_1$ ,  $v_2$ ,  $c_1$ , and  $c_2$  in Fig. 2).

Within Tamm-Dancoff approximation and static screening limit in the  $e-h$  interaction, the energy of the lowest triplet exciton is 1.32 eV. There are two types of triplet excitons in sexithiophene crystal, Frenkel type and charge-transfer type, as shown in Fig. 5 for their spatial distribution. The lowest two triplet levels at 1.32 and 1.62 eV, which are both fourfold degenerate, are formed by Frenkel excitons. Around 2.05 eV, there are eight nearly degenerate triplet states, including fourfold-degenerate Frenkel excitons and fourfold-degenerate charge-transfer excitons. The binding energy of the Frenkel triplet exciton is 1.6 eV, in contrast to 4 eV for that in the gas-phase sexithiophene molecule. The binding energy of the charge-transfer triplet exciton is 0.6 eV at most and decreases with the increase of triplet energy.

The energies of the lowest singlet and triplet excitons are important parameters that determine the behavior of singlet exciton fission in organic semiconductors. We have known

that TDA and static screening limit in the  $e-h$  interaction can cause about 0.2 (0.5) eV error in the energy of the lowest singlet (triplet) exciton of sexithiophene molecule (Table I). It is quite necessary to check the influence of these two approximations on the excitons in crystal. The lowest singlet and triplet excitons in crystal are both of Frenkel type and localized on a molecule. So we can approximately conduct GW+BSE calculations using a single  $\Gamma$  point for them instead of the dense  $k$ -point grids described above. Table II lists the corresponding results under different approximations.

We can see that using only a  $\Gamma$  point induces 0.19 and 0.15 eV redshifts for the lowest singlet and triplet excitons,

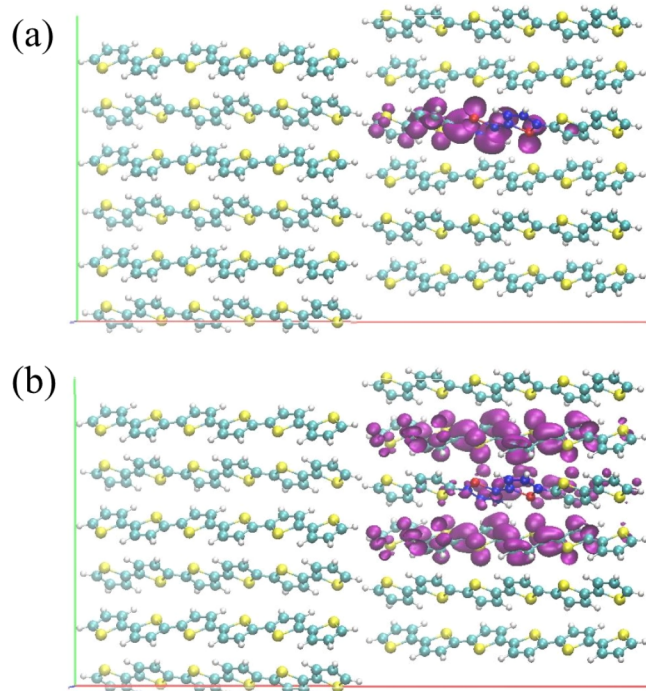


FIG. 5. Electronic charge distribution (purple solid surface) for triplet excitons at the energies of 1.32 (a) and 2.03 eV (b) in a sexithiophene crystal  $1 \times 3 \times 1$  supercell. The hole is fixed near the atoms represented by blue and red balls which are carbon and sulfur atoms, respectively. While it is a Frenkel exciton at 1.32 eV, it is a charge-transfer exciton at 2.03 eV.

TABLE II. Energies (in eV) of the lowest singlet and triplet excitons in sexithiophene crystal calculated with two kinds of  $k$ -point sampling, i.e., a dense one and a  $\Gamma$  only one, under different approximations to the BSE calculations. Please refer to the caption of Table I for details. “dense”:  $k$ -point grids of  $1 \times 2 \times 2$  for matrix elements of dielectric function and self-energy operator, and  $1 \times 7 \times 7$  for the excited state.

$k$ -point	TDA		Full BSE
	sta.	dyn.(1st)	sta.
Singlet			
Dense	1.96	...	...
$\Gamma$	1.77	1.59	1.74
Triplet			
Dense	1.32	...	...
$\Gamma$	1.17	0.67	1.10

respectively. Thus, this is an acceptable approximation. The difference in TDA and full BSE is 0.03 (0.07) eV for the singlet (triplet) exciton, smaller than those in the isolated gas-phase sexithiophene molecule. But the dynamical screening effects in the  $e-h$  interaction are stronger than those in the isolated molecule. This is especially apparent for the triplet exciton where the dynamical correction can amount to 0.5 eV. This can be understood from the ratio between the exciton binding energy of triplet exciton,  $E_B^T$ , and the characteristic plasma frequencies  $\omega_l$  in Eq. (4). The ratio of  $E_B^T$  between isolated molecule and crystal is 2.5, while the ratio of  $\omega_l$  between isolated molecule and crystal can reach 4. This means that the weight of  $E_B^T$  in the denominators of Eq. (4) is more pronounced in crystal than that in isolated molecule.

Here, we cannot give more accurate energies for the lowest singlet and triplet excitons in the sexithiophene crystal at the level of full BSE with dynamical screening in the  $e$ - $h$  interaction due to the huge computational cost. However, we can roughly estimate their energies to be 1.75 and 0.70 eV for the singlet and triplet excitons according to the error that each approximation, including TDA and first-order perturbation approximation in calculating dynamical screening effects of  $e$ - $h$  interaction, introduces. We have discussed above that the DFT-PBE optimized crystal structure can give rise to 0.4 eV redshift of the excitation energies compared to the crystal structure measured by experiment. Taking this further into account, the lowest triplet excited state of sexithiophene crystal should locate around 1.1 eV, which is close to half the energy of the lowest singlet excited state measured by experiment (2.28 eV of the  $a_u$  Davydov component).

## **V. SUMMARY**

In summary, we investigated the electronic excited states and spectroscopic properties of sexithiophene molecule and single crystal with the GW+BSE approach. We found the significant effects of dynamical screening in the electron-hole interaction on the energies of triplet excitons in both the molecule and crystal. We think that it is crucial to consider these effects in first principles calculations to give a reliable picture on the singlet/triplet excited-state energy levels of organic semiconductors. Our calculations reproduce very well

the experimental optical spectra of sexithiophene crystal and the Davydov splitting. There are two types of excitons for both the singlet and triplet states, Frenkel exciton, and charge-transfer exciton. Only the lowest two singlet excitons, which are the degenerate  $a_u$  and  $a_g$  Davydov components, are of Frenkel type with the exciton binding energy of 0.7 eV. The excitons of the  $b_u$  and  $b_g$  Davydov components are of the charge-transfer type with the binding energy of 0.3 eV. The lowest three triplet levels, which are fourfold degenerate, are formed by Frenkel excitons with the binding energy of 1.6 eV. We also speculated that the energy of the lowest triplet exciton is close to half the energy of the lowest singlet exciton, which means that singlet exciton fission may occur in sexithiophene crystal. This work can help us understand in depth the charge transport, energy transfer, and exciton decay processes in sexithiophene and other oligothiophene crystals and films.<sup>14</sup>

#### **ACKNOWLEDGMENTS**

This work was supported by the National Natural Science Foundation of China (Grant Nos. 21173130 and 21433006), the Natural Science Foundation of Shandong Province (Grant No. BS2012CL022), and SRF for ROCS, SEM. Computational resources have been provided by the National Supercomputing Center in Jinan.

- <sup>25</sup>M. L. Tiago, J. E. Northrup, and S. G. Louie, *Phys. Rev. B* **67**, 115212 (2003).
- <sup>26</sup>D. Beljonne, H. Yamagata, J. L. Brédas, F. C. Spano, and Y. Olivier, *Phys. Rev. Lett.* **110**, 226402 (2013).
- <sup>27</sup>P. M. Zimmerman, Z. Zhang, and C. B. Musgrave, *Nat. Chem.* **2**, 648 (2010).
- <sup>28</sup>P. Petelenz and B. Pac, *J. Am. Chem. Soc.* **135**, 17379 (2013).
- <sup>29</sup>P. M. Zimmerman, F. Bell, D. Casanova, and M. Head-Gordon, *J. Am. Chem. Soc.* **133**, 19944 (2011).
- <sup>30</sup>M. Muccini, E. Lunedei, C. Taliani, D. Beljonne, J. Cornil, and J. L. Brédas, *J. Chem. Phys.* **109**, 10513 (1998).
- <sup>31</sup>J. P. Perdew, K. Burke, and M. Ernzerhof, *Phys. Rev. Lett.* **77**, 3865 (1996).
- <sup>32</sup>A. D. Becke, *Phys. Rev. A* **38**, 3098 (1988).
- <sup>33</sup>C. Lee, W. Yang, and R. G. Parr, *Phys. Rev. B* **37**, 785 (1988).
- <sup>34</sup>T. Yanai, D. P. Tew, and N. C. Handy, *Chem. Phys. Lett.* **393**, 51 (2004).
- <sup>35</sup>M. J. Frisch *et al.*, GAUSSIAN 09, Revision B.01, Gaussian, Inc., Wallingford, CT, 2010.
- <sup>36</sup>M. S. José, A. Emilio, D. G. Julian, G. Alberto, J. Javier, O. Pablo, and S.-P. Daniel, *J. Phys.: Condens. Matter* **14**, 2745 (2002).
- <sup>37</sup>L. Hedin, *Phys. Rev.* **139**, A796 (1965).
- <sup>38</sup>L. Hedin and S. Lundqvist, in *Solid State Physics: Advances in Research and Application*, edited by F. Seitz, D. Turnbull, and H. Ehrenreich (Academic, New York, 1969), Vol. 23, p. 1.
- <sup>39</sup>M. S. Hybertsen and S. G. Louie, *Phys. Rev. B* **34**, 5390 (1986).
- <sup>40</sup>Y. Ma, M. Rohlfing, and C. Molteni, *Phys. Rev. B* **80**, 241405 (2009).
- <sup>41</sup>C. Faber, C. Attaccalite, V. Olevano, E. Runge, and X. Blase, *Phys. Rev. B* **83**, 115123 (2011).
- <sup>42</sup>Y. Ma, M. Rohlfing, and C. Molteni, *J. Chem. Theory Comput.* **6**, 257 (2010).
- <sup>43</sup>H. Yin, Y. Ma, J. Mu, C. Liu, and M. Rohlfing, *Phys. Rev. Lett.* **112**, 228301 (2014).
- <sup>44</sup>E. Coccia, D. Varsano, and L. Guidoni, *J. Chem. Theory Comput.* **10**, 501 (2014).
- <sup>45</sup>D. Jacquemin and C. Adamo, *J. Chem. Theory Comput.* **7**, 369 (2011).
- <sup>46</sup>M. J. G. Peach, M. J. Williamson, and D. J. Tozer, *J. Chem. Theory Comput.* **7**, 3578 (2011).
- <sup>47</sup>M. J. G. Peach and D. J. Tozer, *J. Phys. Chem. A* **116**, 9783 (2012).
- <sup>48</sup>M. Knupfer, T. Pichler, M. S. Golden, J. Fink, M. Murgia, R. H. Michel, R. Zamboni, and C. Taliani, *Phys. Rev. Lett.* **83**, 1443 (1999).
- <sup>49</sup>D. Oelkrug, H. J. Egelhaaf, and J. Haiber, *Thin Solid Films* **284–285**, 267 (1996).
- <sup>50</sup>G. Weiser and S. Möller, *Org. Electron.* **5**, 91 (2004).
- <sup>51</sup>E. Cannuccia and A. Marini, *Phys. Rev. Lett.* **107**, 255501 (2011).
- <sup>52</sup>F. Giustino, S. G. Louie, and M. L. Cohen, *Phys. Rev. Lett.* **105**, 265501 (2010).
- <sup>53</sup>C. E. Patrick and F. Giustino, *Nat. Commun.* **4**, 2006 (2013).
- <sup>54</sup>M. Muccini, E. Lunedei, A. Bree, G. Horowitz, F. Garnier, and C. Taliani, *J. Chem. Phys.* **108**, 7327 (1998).
- <sup>55</sup>P. Petelenz and M. Andrzejak, *J. Chem. Phys.* **113**, 11306 (2000).
- <sup>56</sup>G. Horowitz, F. Kouki, A. E. Kassmi, P. Valat, V. Wintgens, and F. Garnier, *Adv. Mater.* **11**, 234 (1999).
- <sup>57</sup>M. A. Loi, A. Mura, G. Bongiovanni, Q. Cai, C. Martin, H. R. Chandrasekhar, M. Chandrasekhar, W. Graupner, and F. Garnier, *Phys. Rev. Lett.* **86**, 732 (2001).
- <sup>58</sup>F. Garnier, G. Horowitz, P. Valat, F. Kouki, and V. Wintgens, *Appl. Phys. Lett.* **72**, 2087 (1998).
- <sup>59</sup>J. W. van der Horst, P. A. Bobbert, M. A. J. Michels, G. Brocks, and P. J. Kelly, *Phys. Rev. Lett.* **83**, 4413 (1999).
- <sup>60</sup>J. W. van der Horst, P. A. Bobbert, P. H. L. de Jong, M. A. J. Michels, G. Brocks, and P. J. Kelly, *Phys. Rev. B* **61**, 15817 (2000).